OPTIMAL INTERPOLATION AND COMPATIBLE RELAXATION IN CLASSICAL ALGEBRAIC MULTIGRID

JAMES BRANNICK, FEI CAO, KARSTEN KAHL, ROBERT D. FALGOUT AND XIAOZHE HU

ABSTRACT. In this paper, we consider a classical algebraic multigrid (AMG) form of *optimal interpolation* that directly minimizes the two-grid convergence rate and compare it with a so-called *ideal interpolation* that minimizes a *weak approximation property* of the coarse space. We study compatible relaxation type estimates for the quality of the coarse grid and derive a new sharp measure using optimal interpolation that provides a guaranteed lower bound on the convergence rate of the resulting two-grid method for a given grid. In addition, we design a generalized bootstrap algebraic multigrid setup algorithm that computes a sparse approximation to the optimal interpolation matrix. We demonstrate numerically that the BAMG method with sparse interpolation matrix (and spanning multiple levels) converges faster than the two-grid method with the standard ideal interpolation (a dense matrix) for various scalar diffusion problems with highly varying diffusion coefficient.

1. INTRODUCTION

We analyze algebraic multigrid (AMG) algorithms for linear systems of algebraic equations

$$A\mathbf{u} = \mathbf{f}, \tag{1.1}$$

coming from cell-centered finite volume discretizations of the scalar elliptic diffusion problem

$$\begin{cases} -\nabla \cdot (a(x)\nabla u) = f & \text{in } \Omega \\ u = 0 & \text{on } \partial\Omega \end{cases} \tag{1.2}$$

where $\Omega = [0,1] \times [0,1]$. The discrete solution and right-hand side satisfy $\mathbf{u}, \mathbf{f} \in \mathbb{R}^{\mathbf{n}}$ and $A \in \mathbb{R}^{n \times n}$ is a symmetric and positive definite matrix. We consider the case where the diffusion coefficient $a(x)$ is highly oscillatory, which is a problem that motivated the design of the original AMG setup algorithm [5, 6].

Multigrid methods are composed of two complimentary processes: *smoothing* (*relaxation*) and *coarse-level correction*. The smoother is usually a simple method like Gauss-Seidel that is traditionally designed to target high-frequency error components, while the coarse-level correction traditionally targets lower-frequency (smooth) error components. In geometric multigrid, the coarse-level correction is defined first, then the smoother is designed to damp the remaining error components. This idea is applied recursively to solve each successive coarse-level equation until the coarsest level is small. A key goal in multigrid research is for the resulting method to be $O(n)$, where n is the number of unknowns in the system.

AMG methods are multigrid methods that generally use only the information in the linear system of equations (1.1). In this paper, we denote the smoother by the error propagator $I - M^{-1}A$. Likewise, the coarse-level correction error propagator is given by $I - \Pi_A(P)$, where $\Pi_A(P) = PA_c^{-1}P^TA$, $P \in \mathbb{R}^{n \times n_c}$ is the interpolation matrix, and $A_c = P^TAP$ is the Galerkin variational coarse-level matrix. The notation $\Pi_A(P)$ indicates an A-orthogonal

projection onto range(P) (we generalize this notation later in the paper). With this, the error propagation matrix of the resulting two-level method reads

$$E_{TG}(P) = (I - M^{-1}A)(I - \Pi_A(P)). \tag{1.3}$$

Unlike geometric multigrid methods, in AMG the smoother is defined first and then interpolation P is constructed in an automated setup algorithm that takes as input the system matrix A and computes P and A_c. The main task in the AMG setup algorithm is thus to construct a *stable* interpolation matrix P such that an *approximation property* holds and both P and A_c are *sparse* matrices. The latter sparsity requirement implies that the procedure can be applied recursively in order to construct an $O(n)$ multilevel solver.

Numerous setup algorithms have been developed for constructing matrix-dependent interpolation, going back to the original classical AMG algorithm [5, 6]. Generally speaking, the setup algorithm for constructing P can be separated into three tasks:

(1) Choosing the set of coarse variables, C, with cardinality $n_c = |C|$.
(2) Determining the nonzero sparsity structure of P.
(3) Computing the values of the nonzero entries in P.

Oftentimes, steps (1) and (2) of the setup algorithm are combined into a single step, as in smoothed aggregation AMG (SA) [22] where the choice of aggregates also determines the sparsity structure of the columns of P. The coefficients of the columns of P are then chosen to approximate certain error components that the smoother cannot treat efficiently, assumed in most cases to be error that is dominated by the eigenvectors of the system matrix with small eigenvalues. In other approaches, e.g., classical AMG, steps (1)-(3) are implemented in different stages within the setup algorithm [5]. Specifically, the notion of strength of coupling between *neighboring* unknowns is used in a maximal independent set algorithm to choose the coarse variable set C. Next, the strongly and weakly coupled neighbors of each of the fine degrees of freedom are determined and, finally, the coefficients of the corresponding row of interpolation are computed in a way that ensures that components of the error (e.g., the constant vector) are well approximated locally. We note that in both approaches, once the coarse degrees of freedom C and the entries of the interpolation matrix P are selected they are fixed and the setup algorithm proceeds to construct the next coarser level. In this way, the algorithm is applied recursively without any measure of the quality of the resulting coarse space in approximating the error in the current solution for the fine-level equations.

Compatible relaxation (CR) [1, 7, 16] and adaptive [12, 13] and bootstrap AMG [2, 4, 8, 9, 10] were introduced as techniques to modify and adjust the coarse variable set and interpolation, respectively. The basic idea in these approaches is to develop local measures to assess the suitability of the computed coarse space for a given problem. Although these approaches have been successfully developed and extended to handle numerous applications, theoretical issues remain unresolved. For example, although the convergence rate of the F-relaxation form of CR that is typically used in practice does give a qualitative measure of the suitability of the coarse set, it does not accurately predict the convergence rate of the resulting two-grid solver with ideal interpolation in general (see [3, 7]). Moreover, the so-called ideal interpolation matrix used as the basis of CR does not in general give the fastest possible convergence rate of the two-level method over all possible choices of P and, hence, it may not provide a reliable measure of the quality of the coarse variable set for certain challenging problems.

In this paper, we study these issues further with the aim of gaining a deeper understanding of AMG from theoretical and practical points of view. In Section 2, we derive an optimal interpolation matrix $P_\sharp$ (Lemma 1) and its corresponding classical AMG form $\tilde{P}_\sharp$. We then extend the theoretical framework in [16] to include $\tilde{P}_\sharp$ by generalizing the definition of ideal interpolation (Lemma 2) and defining the coarse variables associated with $\tilde{P}_\sharp$ (Lemma 3). Section 3.1 introduces measures of the quality of the coarse grid based on ideal interpolation, optimal $\tilde{P}_\sharp$, and the notion of compatible relaxation [1, 7]. Regarding the ideal interpolation variant, we derive a practical approach for estimating the convergence rate of the resulting two-grid method directly so that the CR convergence rate is not needed in this setting. In addition, this section contains the derivation of a generalized bootstrap AMG (BAMG) setup algorithm that aims to build a sparse interpolation matrix P based on approximating the optimal (but possibly dense) $\tilde{P}_\sharp$. Section 4 contains numerical results that illustrate our findings and new algorithms for various scalar diffusion test problems. Numerically, we show that the reliability and robustness of CR depends critically on the choice of the coarse variables and that when the standard simple form of CR is used, the resulting estimates of the two-grid solver are not sharp in general. Moreover, we show that our direct approach approach for computing two-grid convergence with ideal interpolaiton does give quantitatively accurate estimates. In addition, we show that the new generalized BAMG method with sparse P (and spanning multiple levels) converges faster than the two-grid method with the standard ideal interpolation (possibly a dense matrix) for our test problems. We note that our new generalized BAMG method represents a first attempt to build an AMG algorithm based on $\tilde{P}_\sharp$, the optimal classical AMG form of interpolation.

2. Two-level theory and optimal interpolation

In Theorem 4.3 in [15], the following identity for the convergence rate of the two-level method is introduced

$$\|E_{TG}(P)\|_A^2 = 1 - \frac{1}{\sup_{\mathbf{v}} \kappa(P,\mathbf{v})}, \quad \kappa(P,\mathbf{v}) = \frac{\|(I - \Pi_{\widetilde{M}}(P))\mathbf{v}\|_{\widetilde{M}}^2}{\|\mathbf{v}\|_A^2}, \tag{2.1}$$

where $\Pi_{\widetilde{M}}(P) = P(P^T\widetilde{M}P)^{-1}P^T\widetilde{M}$ is the $\langle\cdot,\cdot\rangle_{\widetilde{M}}$ orthogonal projection onto range(P), where $\langle \mathbf{x},\mathbf{y}\rangle_{\widetilde{M}} := \langle \widetilde{M}\mathbf{x},\mathbf{y}\rangle$ denotes the $\widetilde{M}$ inner product, with $\widetilde{M}^{-1} = M^{-1} + M^{-T} - M^{-T}AM^{-1}$ denoting the symmetrized smoother, so that $\widetilde{M} = M(M + M^T - A)^{-1}M^T$. Note that, assuming $M + M^T - A$ is symmetric and positive definite (SPD) is equivalent to assuming the convergence of the chosen smoother defined by M.

Using (2.1) it is straightforward to derive the optimal two-grid convergence rate $\|E_{TG}(P)\|_A^2$ with respect to P, for a given smoother M. We note that this result is found in [15] (see Corollary 4.1) and more recently in the review paper [25]. From this general form of optimal P we then derive a classical AMG form of optimal P via a post-scaling, which is the result of primary interest in this paper. In particular, we focus on studying this classical AMG form of optimal interpolation and comparing it in a practical setting with the so-called ideal interpolation.

Lemma 1. *Let $P : \mathbb{R}^{n_c} \to \mathbb{R}^n$ be full rank and let $\lambda_1 \le \lambda_2 \le \ldots \le \lambda_n$ and $\mathbf{v}_1, \mathbf{v}_2, \ldots, \mathbf{v}_n$ denote the eigenvalues and orthonormal (w.r.t $\langle\cdot,\cdot\rangle_{\widetilde{M}}$ for convenience of representation) eigenvectors of the generalized eigenvalue problem*

$$A\mathbf{x} = \lambda\widetilde{M}\mathbf{x}. \tag{2.2}$$

Also to simplify notation we use $(A, \widetilde{M})$ to represent the above generalized eigenvalue problem 2.2. Then the minimal convergence rate of the two-grid method is given by

$$\|E_{TG}(P_\sharp)\|_A^2 = 1 - \frac{1}{\kappa_\sharp}, \quad \kappa_\sharp := \inf_{\dim(\mathrm{range}(P)) = n_c} \sup_v \kappa(P, \mathbf{v}) = \frac{1}{\lambda_{n_c+1}}, \tag{2.3}$$

where the optimal interpolation operator $P_\sharp$ satisfies

$$\mathrm{range}(P_\sharp) = \mathrm{range}(\begin{pmatrix}\mathbf{v}_1 & \mathbf{v}_2 & \cdots & \mathbf{v}_{n_c}\end{pmatrix}). \tag{2.4}$$

For sake of definiteness we set $P_\sharp = \begin{pmatrix}\mathbf{v}_1 & \mathbf{v}_2 & \cdots & \mathbf{v}_{n_c}\end{pmatrix}$ throughout the paper.

Proof. Starting with the equality in (2.1) first observe that if we denote $\mathcal{P} = \mathrm{range}(P)$ and its $\widetilde{M}$-orthogonal complement by $\mathcal{S}$ we find that for any P

$$\frac{1}{\sup_{\mathbf{v}} \kappa(P, \mathbf{v})} = \inf_{\mathbf{v}} \frac{\|\mathbf{v}\|_A^2}{\|(I - \Pi_{\widetilde{M}}(P))\mathbf{v}\|_{\widetilde{M}}^2} \leq \inf_{\mathbf{v} \in \mathcal{S}} \frac{\|\mathbf{v}\|_A^2}{\|\mathbf{v}\|_{\widetilde{M}}^2}.$$

Thus, we obtain for any P that

$$\|E_{TG}(P)\|_A^2 \geq 1 - \inf_{\mathbf{v} \in \mathcal{S}} \frac{\|\mathbf{v}\|_A^2}{\|\mathbf{v}\|_{\widetilde{M}}^2}$$

Finally due to $\dim(\mathcal{S}) + \dim(\mathcal{P}) = n$ we get

$$\inf_{\dim(\mathcal{P}) = n_c} \|E_{TG}(P)\|_A^2 \geq 1 - \sup_{\dim(\mathcal{S}) = n - n_c} \inf_{\mathbf{v} \in \mathcal{S} \setminus \{0\}} \frac{\|\mathbf{v}\|_A^2}{\|\mathbf{v}\|_{\widetilde{M}}^2}.$$

Based on Courant-Fischer Min-max representation, we obtain:

$$\inf_{\dim(\mathcal{P}) = n_c} \|E_{TG}(P)\|_A^2 \geq 1 - \lambda_{n_c+1}.$$

The equality in this bound is obtained by setting $\mathcal{S} = \mathcal{S}_\sharp = \mathrm{range}(\begin{pmatrix}\mathbf{v}_{n_c+1} & \mathbf{v}_{n_c+2} & \cdots & \mathbf{v}_n\end{pmatrix})$. Now, since $\mathcal{P}$ is the $\widetilde{M}$-orthogonal complement of $\mathcal{S}$, it follows that $P = P_\sharp$ and

$$\|E_{TG}(P_\sharp)\|_A^2 = 1 - \lambda_{n_c+1}.$$

Finally, the optimal convergence rate for the two-grid method is obtained by choosing any interpolation that has the same range as $P_\sharp$, namely, by setting

$$P = P_\sharp Z, \quad \text{where we assume} \quad Z^{-1} \quad \text{exists.}$$

In this way, one obtains the same optimal convergence rate since by direct computation

$$\begin{aligned} E_{TG}(P_\sharp Z) &= (I - M^{-1}A)(I - P_\sharp Z((P_\sharp Z)^T A P_\sharp Z)^{-1}(P_\sharp Z)^T A) \\ &= (I - M^{-1}A)(I - P_\sharp((P_\sharp)^T A P_\sharp)^{-1}(P_\sharp)^T A) = E_{TG}(P_\sharp). \end{aligned}$$

□

We note that the above identity for the projection on $P_\sharp$ holds for $\Pi_X(P_\sharp)$ as well, where X is assumed to be any SPD matrix. This is summarized in the following corollary.

Corollary 1. *Any projection $\Pi_X(P) = P(P^T X P)^{-1} P^T X$ is invariant with respect to post-multiplication of interpolation P by an invertible matrix Z, $P \leftarrow PZ$. Here X is assumed to be any SPD matrix.*

Proof. The proof is identical to the derivation for $E_{TG}(P_\sharp Z)$, where the system matrix A is replaced by X and the smoother is omitted. □

In order to derive a classical AMG form of the optimal interpolation $P_\sharp$, we use the result from the last lemma that the spectral radius of E_{TG} remains unchanged if we replace $P_\sharp$ by $P_\sharp Z$ for any nonsingular (invertible) matrix Z. The classical AMG form of interpolation, assuming a splitting of the fine-level degrees of freedom into C and F, is given by

$$P = \begin{bmatrix} W \\ I \end{bmatrix} \begin{matrix} \} F \\ \} C \end{matrix}, \tag{2.5}$$

where $C \subset \{1, ..., n\}$ and $F = \{1, ..., n\} \setminus C$, and $W \in \mathbb{R}^{|F|\times|C|}$ defines the interpolation weights. Thus, if we reorder the optimal interpolation matrix so that it has the form

$$P_\sharp = \begin{bmatrix} P_f \\ P_c \end{bmatrix}, \tag{2.6}$$

such that P_c is non-singular, then it follows that the interpolation matrix

$$\tilde{P}_\sharp = P_\sharp P_c^{-1} = \begin{bmatrix} \tilde{W} \\ I \end{bmatrix}, \quad \tilde{W} = P_f P_c^{-1} \tag{2.7}$$

also minimizes $\sup_{\mathbf{v}\neq 0} \kappa(\mathbf{v})$.

The interpolation matrices $P_\sharp$ and $\tilde{P}_\sharp$ are in general not of direct use in practice since they require the computation of n_c eigenvectors of the generalized eigenproblem in (2.2) and they are typically dense matrices. In the remainder of this section, we make various connections between $\tilde{P}_\sharp$ and existing two-grid theory used in deriving classical AMG forms of interpolation. Then, in the next section, we consider designing practical algorithms that use $\tilde{P}_\sharp$.

2.1. **An approximation property and ideal interpolation.** AMG approaches for constructing interpolation P are based on an approximation property of the coarse space, which is formulated as

$$\mu_X(PR) := \sup_{\mathbf{v}} \frac{\|(I - PR)\mathbf{v}\|_X^2}{\|\mathbf{v}\|_A^2} \leq \eta \ \forall \mathbf{v} \in \mathbb{R}^n, \tag{2.8}$$

where $R : \mathbb{R}^n \to \mathbb{R}^{n_c}$ defines the coarse variables, i.e,. $u_c = Ru$, and must be chosen such that $RP = I$ and the matrix $X \in \mathbb{R}^{n\times n}$ is symmetric positive definite. Note that the left side in (2.8) will precisely determine the convergence rate in (2.1) if $X = \widetilde{M}$ and $R = (P^T\widetilde{M}P)^{-1}P^T\widetilde{M}$. If X is not equal to $\widetilde{M}$, but is instead bounded from above such that for some constant σ

$$\langle \widetilde{M}\mathbf{v}, \mathbf{v}\rangle = \|\mathbf{v}\|_*^2 \leq \sigma\langle X\mathbf{v}, \mathbf{v}\rangle, \tag{2.9}$$

then

$$\|(I - \Pi_{\widetilde{M}}(P))\mathbf{v}\|_{\widetilde{M}}^2 \leq \|(I - PR)\mathbf{v}\|_{\widetilde{M}}^2 \leq \sigma\|(I - PR)\mathbf{v}\|_X^2.$$

As a consequence, the two-level method is a uniform contraction in $\|\cdot\|_A$-norm *if* η is uniformly bounded for some X such that (2.9) holds. A typical choice for X is $X = D$ (the diagonal of A).

The approximation property (2.8) is used in [16] to establish a theoretical framework for building AMG algorithms that incorporates general smoothers (especially non-pointwise smoothers), coarsening approaches, and compatible relaxation methods for measuring coarse-grid quality. An important feature of the framework is the use of the operator R to both define and generalize the notion of *coarse variables* [1]. Once R is specified, μ_X in (2.8)

serves as a metric for measuring the quality of the interpolation operator P. The goal in practice is to minimize μ_X while maintaining sparsity in P. The absolute minimizer is called *ideal interpolation* in this paper (see Lemma 2 below) and is denoted by $P_\star$. Although $P_\star$ is usually not sparse, it often serves as a good "target" interpolation operator that can be used to generate a variety of practical approaches for building P.

In the classical AMG setting, the coarse variables are a subset of the fine variables. That is, in the context of the above framework,

$$R = \begin{bmatrix} 0 & I \end{bmatrix}, \quad S = \begin{bmatrix} I \\ 0 \end{bmatrix}, \tag{2.10}$$

and interpolation P has the form given in (2.5), hence $RS = 0$ and $RP = I$. Here, the unknowns are assumed to be ordered so that the matrix has the block form

$$A = \begin{bmatrix} A_{ff} & A_{fc} \\ A_{cf} & A_{cc} \end{bmatrix} \begin{matrix} \} F \\ \} C \end{matrix}. \tag{2.11}$$

In this setting, ideal interpolation is then given by

$$P_\star = P_\circ \equiv \begin{bmatrix} W_\circ \\ I \end{bmatrix}, \quad W_\circ = -A_{ff}^{-1} A_{fc}\,. \tag{2.12}$$

We note that the coarse-grid matrix $A_c = P_\circ^T A P_\circ = A_{cc} - A_{cf} A_{ff}^{-1} A_{fc}$ is the usual Schur complement that one obtains for the given C/F splitting.

For this simple choice of R, many practical approaches have been developed for constructing P based on approximating $P_\circ$ and compatible relaxation is also fairly straightforward. However, $P_\circ$ is different in general from the optimal $P_\sharp$ and, as we show in the numerics section, this difference can lead to substantial changes in convergence rates of the resulting two-grid method in certain cases.

From (2.1) and Lemma 1, a better choice for coarse variables is given by $R = R_\sharp := P_\sharp^T \widetilde{M}$. Here, the measure $\mu_{\widetilde{M}}$ in (2.8) is exact and the minimal convergence rate of the two-grid method is achievable with $P = P_\star = P_\sharp$. However, this choice of R is less intuitive and, although it also induces the classical AMG form $\tilde{P}_\sharp$ in (2.7) (by Corollary 1), the theory in [16] does not cleanly encompass this setting due to an orthogonality assumption on R (see Corollary 3.2). In Lemma 2, we generalize the formula for $P_\star$ presented in [16] so that $\tilde{P}_\sharp$ is represented naturally in the theory. In Lemma 3, we then define the $\tilde{R}_\sharp$ that generates $\tilde{P}_\sharp$, and we show that the new formula for $P_\star$ and all of the theoretical requirements are satisfied. Together, Lemmas 1–3 provide an optimal framework for guiding the development of AMG algorithms of classical type.

Lemma 2. *Let R be given and satisfy $RP = I$. Define $S : \mathbb{R}^{n_f} \to \mathbb{R}^n$, where $n_f = n - n_c$ such that $RS = 0$. Then, ideal interpolation is the solution to the* min-max *problem $\mu_X^\star = \min_P \mu_X(PR)$ and is given by*

$$P_\star := (I - \Pi_A(S))Z_* = (I - S(S^T AS)^{-1} S^T A) Z_\star \tag{2.13}$$

where $P_\star$ satisfies (by definition) $P_\star^T AS = 0$, $Z_\star : \mathbb{R}^{n_c} \to \mathbb{R}^n$ is full rank such that $RZ_\star = I$, and we can take $Z_\star = R^T(RR^T)^{-1}$. Further, the corresponding minimum has the closed form

$$\mu_X^\star = \frac{1}{\lambda_{\min}((S^T XS)^{-1}(S^T AS))}. \tag{2.14}$$

In order to minimize the measure μ_X with respect to P, the only requirement that ideal interpolation $P_\star$ needs to satisfy, apart from the usual requirements that $RP_\star = I$ and $RS = 0$, is the condition that $P_\star^T AS = 0$ (see Equation (3.9) in [16]). This condition in turn is satisfied for the choice above involving the A-orthogonal projection onto range(S). Moreover, if we consider the condition $RP_\star = I$, we find that (since $RS = 0$)

$$RP_\star = R(I - \Pi_A(S))Z_\star = RZ_\star = I. \tag{2.15}$$

The choice $Z_\star = R^T(RR^T)^{-1}$ satisfies (2.15) and is orthogonal to null(R) = range(S). In [16], the formula for $P_\star$ assumes that R is normalized such that $RR^T = I$, which limits the operators that can be represented. We show below that this limitation includes $\tilde{P}_\sharp$.

Lemma 3. *For $P = \tilde{P}_\sharp$ and $X = \widetilde{M}$ one obtains, in light of Lemmas 1 and 2, that*

$$\tilde{R}_\sharp = (\tilde{P}_\sharp P_c P_c^T)^T \widetilde{M}, \quad S_\sharp = \begin{pmatrix} \mathbf{v}_{n_c+1} & \cdots & \mathbf{v}_n \end{pmatrix} \tag{2.16}$$

and

$$\mu_{\widetilde{M}}^\sharp := \frac{1}{\lambda_{\min}((S_\sharp^T \widetilde{M} S_\sharp)^{-1}(S_\sharp^T A S_\sharp))} = \frac{1}{\lambda_{n_c+1}}. \tag{2.17}$$

For these choices of $R = \tilde{R}_\sharp$, $S = S_\sharp$, and $P = \tilde{P}_\sharp$, we have that $\tilde{R}_\sharp \tilde{P}_\sharp = I$ and $\tilde{R}_\sharp S_\sharp = 0$, so that the assumptions of Lemma 2 hold. Moreover, $\tilde{P}_\sharp \tilde{R}_\sharp = \Pi_{\widetilde{M}}(\tilde{P}_\sharp) = \Pi_A(\tilde{P}_\sharp)$ and the resulting ideal P obtained from minimizing the measure in (2.8) *has the same form as the optimal one, namely*

$$P_\star = (I - S_\sharp(S_\sharp^T A S_\sharp)^{-1} S_\sharp^T A)Z_\star = \Pi_{\widetilde{M}}(\tilde{P}_\sharp)Z_\star = \tilde{P}_\sharp(\tilde{R}_\sharp Z_\star) = \tilde{P}_\sharp, \tag{2.18}$$

where $P_\star$ is defined in Lemma 2.

Proof. The result in (2.18) is established by noting that $S_\sharp^T \widetilde{M} S_\sharp = I$ and

$$S_\sharp^T A S_\sharp = \operatorname{diag}(\lambda_{n_c+1}, \ldots, \lambda_n) = \Lambda_{S_\sharp},$$

implying

$$S_\sharp^T \widetilde{M} = (\widetilde{M} S_\sharp)^T = (A S_\sharp \Lambda_{S_\sharp}^{-1})^T = \left(S_\sharp^T A S_\sharp\right)^{-1} S_\sharp^T A.$$

Hence,

$$\Pi_{\widetilde{M}}(S_\sharp) = S_\sharp(S_\sharp^T \widetilde{M} S_\sharp)^{-1} S_\sharp^T \widetilde{M} = S_\sharp S_\sharp^T \widetilde{M} = S_\sharp \left(S_\sharp^T A S_\sharp\right)^{-1} S_\sharp^T A = \Pi_A(S_\sharp).$$

Likewise, one can show that $\tilde{P}_\sharp \tilde{R}_\sharp = \Pi_{\widetilde{M}}(P_\sharp) = \Pi_A(P_\sharp)$. From Corollary 1, we also have that $\tilde{P}_\sharp \tilde{R}_\sharp = \Pi_{\widetilde{M}}(\tilde{P}_\sharp) = \Pi_A(\tilde{P}_\sharp)$. Now, since $I - \Pi_{\widetilde{M}}(S_\sharp) = \Pi_{\widetilde{M}}(P_\sharp)$, which follows by definition, we have

$$P_\star = (I - S_\sharp(S_\sharp^T A S_\sharp)^{-1} S_\sharp^T A)Z_\star = \Pi_{\widetilde{M}}(P_\sharp)Z_\star = \Pi_{\widetilde{M}}(\tilde{P}_\sharp)Z_\star = \tilde{P}_\sharp(\tilde{R}_\sharp Z_\star) = \tilde{P}_\sharp,$$

where $\tilde{R}_\sharp Z_\star = I$ by (2.15). Thus, if one chooses the optimal forms $R = \tilde{R}_\sharp$, $S = S_\sharp$ and $X = \widetilde{M}$, then the measure in (2.8) also has as its minimizer the optimal form of interpolation $P_\sharp$ given in Lemma 1. □

With the $\tilde{R}_\sharp$ given in (2.16), it is easy to see that

$$\tilde{R}_\sharp \tilde{R}_\sharp^T = (\tilde{P}_\sharp P_c P_c^T)^T \widetilde{M} \widetilde{M} (\tilde{P}_\sharp P_c P_c^T) = P_c P_\sharp^T \widetilde{M}^2 P_\sharp P_c^T \neq I.$$

Furthermore, if we set $\hat{R}_\sharp = (\tilde{R}_\sharp \tilde{R}_\sharp^{\,T})^{-1/2}\tilde{R}_\sharp$ so that $\hat{R}_\sharp \hat{R}_\sharp^{\,T} = I$, then $\hat{R}_\sharp \tilde{P}_\sharp = (\tilde{R}_\sharp \tilde{R}_\sharp^{\,T})^{-1/2} \neq I$. Hence, from this example we see that the $P_\star$ construction in [16] is not general enough to cover the results in the previous lemma.

Another interesting aspect of $\tilde{R}_\sharp$ in (2.16) is that it provides a representation of coarse variables that is somewhat easy to understand and use for algorithm development. Noting that $P_c = [0\ I]P_\sharp$, we have that

$$\tilde{R}_\sharp = P_c P_\sharp^T \widetilde{M} = [0\ I]\ \Pi_{\widetilde{M}}(P_\sharp).$$

Hence, the coarse variables in this setting are an $\widetilde{M}$-orthogonal projection of the fine variables onto the space spanned by the smallest eigenmodes (i.e., eigenvectors with smallest eigenvalues) of the generalized eigenvalue problem in (2.2), restricted to C-points.

We note that $P_\star$ is also optimal in terms of energetic stability in the following sense. From [16], assuming that the coarse variables have been constructed so that $\mu^\star_{\widetilde{M}}$ is bounded for all $\mathbf{v} \neq 0$, then using a P that satisfies the following stability property also implies convergence of the resulting two-level method

$$\langle APR\mathbf{v},\ PR\mathbf{v}\rangle \leq \beta\,\langle A\mathbf{v},\ \mathbf{v}\rangle \quad \forall\,\mathbf{v}, \tag{2.19}$$

where $\beta \geq 1$ is a constant. This more general result is interesting because it allows for various approaches of defining interpolation. Moreover, it separates the tasks of selecting the coarse variables and defining interpolation. We note that (2.19) has been used extensively in the literature [20, 23, 11] to derive various techniques for constructing an energetically stable P. We also have from Lemma 3 that with $P = \tilde{P}_\sharp$, $R = \tilde{R}_\sharp$, and $S = S_\sharp$, such that $\mu^\star_{\widetilde{M}} = \frac{1}{\lambda_{n_c+1}}$, then it follows that $\tilde{P}_\sharp \tilde{R}_\sharp = \Pi_{\widetilde{M}}(\tilde{P}_\sharp) = \Pi_A(\tilde{P}_\sharp)$ so that $\beta = \beta_\sharp = 1$ in (2.19), which is of course the minimal value since $\Pi_A(\tilde{P}_\sharp)$ is the A-orthogonal projection onto range$(\tilde{P}_\sharp)$.

3. Bootstrap AMG and optimal interpolation

3.1. **Compatible relaxation and optimal interpolation.** Here, we introduce the notion of compatible relaxation (CR) and show how the process can be used to obtain a bound on the convergence rate of the two-grid method with ideal interpolation, namely we present a bound on $\mu^\star_{\widetilde{M}}$ that uses the convergence rate of CR. The resulting bound in turn gives a measure of the quality of the coarse variable set, since it shows that, for the given set C there exists an interpolation matrix (the ideal one) such that the two-grid method convergence is acceptable. We then consider CR in terms of $\tilde{R}_\sharp$ and $S_\sharp$ defined in Lemma 3 and contrast this approach to the more practical choices that have been considered in our previous studies of this topic.

Compatible relaxation, as defined by Brandt [1], is *a modified relaxation scheme that keeps the coarse-level variables invariant*. Generally, the compatible relaxation iteration is defined as

$$\mathbf{v}_{k+1} = (I - SM_S^{-1}S^T A)\mathbf{v}_k, \tag{3.1}$$

where $M_S = S^T M S$ and, as in Lemma 2, we assume that R and S are chosen such that $RS = 0$. Note that from this assumption it follows that $R\mathbf{v}_{k+1} = R\mathbf{v}_k$ and thus we can consider compatible relaxation in the L_2 complementary space, leading to an iteration of the form

$$\mathbf{v}_{k+1} = (I - M_S^{-1}A_S)\mathbf{v}_k, \tag{3.2}$$

where $A_S = S^T A S$. Now, the convergence rate of this iteration is related to the measure $\mu^{\star}_{\widetilde{M}}$ in (2.14) as follows

$$\mu^{\star}_{\widetilde{M}} \leq \frac{\Delta^2}{1-\rho_S}. \tag{3.3}$$

Here, $\Delta \geq 1$ measures the deviation of M from its symmetric part (see [16]) and

$$\rho_S = \left\| (I - M_S^{-1} A_S) \right\|_{A_S}. \tag{3.4}$$

Note that, although we use ρ to represent the spectral radius of a matrix, the quantity ρ_S is in general only an upper bound for the spectral radius of compatible relaxation; it is equal to the spectral radius when M is symmetric. For this reason, we work with the symmetrized Gauss Seidel smoother $\widetilde{M}$ in all cases, which gives $\Delta = 1$ in the above bound.

If iteration (3.2) is fast to converge, then $\mu^{\star}_{\widetilde{M}}$ is bounded, that is, fast convergence of CR implies a coarse variable set of good quality and the existence of a P such that the resulting two-level method is uniformly convergent. One can then estimate the value of ρ_s in (3.4) in practice by running the compatible relaxation iteration in (3.2) and monitoring its convergence.

In the classical AMG setting, given a choice of the coarse and fine variable sets, C and F, and assuming that R and S are defined as in (2.10) we have that the iteration in (3.2) reduces to simple F-relaxation

$$\mathbf{v}_{k+1} = (I - M_{ff}^{-1} A_{ff}) \mathbf{v}_k, \tag{3.5}$$

which is straightforward to compute. We note that though this variant of CR is user-friendly, it has been observed in practice that its spectral radius does not provide an accurate prediction of the convergence rate of the two-level method with ideal interpolation in some cases [11]. Thus, the bound in (3.3) may not be sharp for such problems.

When $P = P_\circ, W_\circ = -A_{ff}^{-1} A_{fc}$ as in (2.12) and R and S are defined as in (2.10), it is easy to show that

$$I - \Pi_A(P_\circ) = I - P_\circ (P_\circ^T A P_\circ)^{-1} P_\circ^T A = S (S^T A S)^{-1} S^T A = \begin{pmatrix} I & -W_\circ \\ 0 & 0 \end{pmatrix}. \tag{3.6}$$

This result implies that the spectral radius of the two-grid error propagator, $\rho(E_{TG}(P_\circ))$, can be accurately estimated in practice if an estimate of A_{ff}^{-1} is available. Moreover, the fast convergence of the F-relaxation form of CR in (3.5) implies that A_{ff} is well conditioned and (as we show later in the numerical experiments) that A_{ff}^{-1} can be efficiently estimated using a polynomial approximation [11]. In particular, if we consider compatible relaxation defined by (3.2) and assume that $\rho_s \leq \delta < 1$, then we have that

$$\kappa(A_{ff}) \leq \kappa(M_{ff}) \frac{1+\delta}{1-\delta}, \tag{3.7}$$

where $\kappa(A)$ is the condition number of the matrix A. In the numerical tests, we use the diagonally scaled preconditioned Conjugate Gradient iteration to compute an approximation to A_{ff}^{-1}.

The approximation obtained by CR can be made optimal if we use the optimal forms of R, S, and P, as defined in Lemma 3. Namely, if we use $\tilde{R}_\sharp$ and $S_\sharp$, and we assume that the

smoother is symmetric Gauss Seidel, then instead of arriving at the F-relaxation form of CR given in (3.5) we have that

$$\widetilde{M}_{S_\sharp} = S_\sharp^T \widetilde{M} S_\sharp = I \quad \text{and} \quad A_{S_\sharp} = S_\sharp^T A S_\sharp = \Lambda_{S_\sharp} := \text{diag}(\lambda_{n_c+1}, ..., \lambda_n), \tag{3.8}$$

where λ_i are the generalized eigenvalues of the eigenproblem involving $(A, \widetilde{M})$. Thus, the spectral radius of the CR error propagation matrix is given by

$$\rho_{S_\sharp}(I - \widetilde{M}_{S_\sharp}^{-1} A_{S_\sharp}) = 1 - \min_i(\Lambda_{S_\sharp})_{ii} = 1 - \lambda_{n_c+1}. \tag{3.9}$$

Here, unlike the simplified version of CR given above, the convergence rate of this form of CR does not depend on the actual coarse points that are chosen, but only on the cardinality of the coarse variable set $n_c = |C|$. However, if we recall the classical AMG form of optimal interpolation given in (2.7):

$$\tilde{P}_\sharp = P_\sharp P_c^{-1} = \begin{bmatrix} \tilde{W} \\ I \end{bmatrix}, \quad \tilde{W} = P_f P_c^{-1}, \tag{3.10}$$

then we observe that P_c used in constructing $\tilde{P}_\sharp$ does depend on the choice of coarse grid points. Hence, in this setting we can use CR to determine the number of coarse points that are required in order to achieve a convergence rate of the resulting two-grid method and then we choose the set C so that P_c is well conditioned. This assumption in turn implies P_c^{-1} is computable in the approximation to $\tilde{P}_\sharp$ and as we show numerically this also tends to produce a local (decaying) optimal interpolation matrix.

3.2. **Generalized bootstrap AMG.** Next, we consider designing a bootstrap AMG setup algorithm that incorporates the generalized eigen-problem in (2.2) to compute test vectors used in constructing least squares interpolation. We note that in the original BAMG setup algorithm developed in [4] the eigen-problem involving only A was used to compute approximate eigenvectors that are provided as input to the least squares process that constructs the interpolation matrix. As we will point out, there are only a few changes that are needed in order to adapt the least squares interpolation and bootstrap multilevel setup to the generalized eigenvalue problem.

3.2.1. *Bootstrap AMG setup.* For definiteness, we provide an outline of the version of the bootstrap AMG setup that was designed and analyzed in [4] and that we use in our tests in section 4. We point out the modifications that are necessary to adjust the components of the method to the generalized eigenvalue problem.

The least squares interpolation matrix used in BAMG is defined to fit collectively a set of test vectors (TVs) that should characterize the eigenvectors with small eigenvectors of the system matrix (or the generalized eigenproblem). Assuming the sets of interpolatory variables, C_i, for each $i \in F$, and a set of test vectors, $\mathcal{V} = \{\mathbf{v}^{(1)}, \ldots, \mathbf{v}^{(k)}\}$, have been determined, the ith row of P, denoted by $\mathbf{p}_i$, is defined as the minimizer of the local least squares problem:

$$\mathcal{L}(\mathbf{p}_i) = \sum_{\kappa=1}^{k} \omega_k \left(\mathbf{v}_{\{i\}}^{(\kappa)} - \sum_{j \in C_i} (\mathbf{p}_i)_j \, \mathbf{v}_{\{j\}}^{(\kappa)} \right)^2 \to \min . \tag{3.11}$$

Here, the notation $\mathbf{v}_{\widetilde{\Omega}}$ denotes the canonical restriction of the vector $\mathbf{v}$ to the set $\widetilde{\Omega} \subset \Omega$, e.g., $\mathbf{v}_{\{i\}}$ is simply the ith entry of $\mathbf{v}$. Conditions on the uniqueness of the solution to

minimization problem (3.11) and an explicit form of the minimizer have been derived in [4]. In contrast to the original least squares interpolation we choose the weights $\omega_\kappa > 0$ by

$$\omega_\kappa = \frac{\|\mathbf{v}^{(\kappa)}\|_X}{\|\mathbf{v}^{(\kappa)}\|_A}.$$

In the original formulation $X = I$ corresponds to the inverse Rayleigh-Quotient of $\mathbf{v}^{(\kappa)}$. Choosing $X = \widetilde{M}$ the weight is the inverse generalized Rayleigh-Quotient w.r.t. the pencil $(A, \widetilde{M})$.

The test vectors used in the least squares process are computed using a bootstrap multilevel setup cycle. The algorithm begins with relaxation applied to the homogenous system,

$$A_l \mathbf{x}_l = 0, \tag{3.12}$$

on each grid, $l = 0, ..., L-1$; assuming that a priori knowledge of the algebraically smooth error is not available, these vectors are initialized randomly on the finest grid, whereas on all coarser grids they are defined by restricting the existing test vectors computed on the previous finer grid.

Once an initial MG hierarchy has been computed, the current sets of TVs are further enhanced on all grids using the existing multigrid structure. Specifically, the given hierarchy is used to formulate a multigrid eigensolver which is then applied to an appropriately chosen generalized eigenproblem to compute additional test vectors. This overall process is then repeated with the current AMG method applied in addition to (or replacing) relaxation as the solver for the homogenous systems in (3.12). Figure 3.1 provides a schematic outline of the bootstrap V- and W-cycle setup algorithms. In general, V^m and W^m denote setup algorithms that use m iterations of the V- and W-cycles, respectively.

The rationale behind the multilevel generalized eigensolver (MGE) is as follows. Assume an initial multigrid hierarchy has been constructed. Given the initial Galerkin operators $A_0, A_1, \ldots, A_L$ on each level and the corresponding interpolation operators $P_{l+1}^l, l = 0, \ldots, L-1$, define the composite interpolation operators as $P_l = P_1^0 \cdot \ldots \cdot P_l^{l-1},\ l = 1, \ldots, L$. Then, for any given vector $x_l \in \mathbb{R}^{n_l}$ we have $\langle \mathbf{x}_l, \mathbf{x}_l \rangle_{A_l} = \langle P_l \mathbf{x}_l, P_l \mathbf{x}_l \rangle_A$. Furthermore, defining $X_l = P_l^T X P_l$ for any X symmetric and positive definite we obtain

$$\frac{\langle \mathbf{x}_l, \mathbf{x}_l \rangle_{A_l}}{\langle \mathbf{x}_l, \mathbf{x}_l \rangle_{X_l}} = \frac{\langle P_l \mathbf{x}_l, P_l \mathbf{x}_l \rangle_A}{\langle P_l \mathbf{x}_l, P_l \mathbf{x}_l \rangle_X}.$$

This observation in turn implies that on any level l, given a vector $\mathbf{x}^{(l)} \in \mathbb{R}^{n_l}$ and $\lambda^{(l)} \in \mathbb{R}$ such that $A_l \mathbf{x}^{(l)} = \lambda^{(l)} X_l \mathbf{x}^{(l)}$, its Rayleigh quotient (RQ) fullfills

$$\mathrm{rq}(P_l \mathbf{x}^{(l)}) := \frac{\langle P_l \mathbf{x}^{(l)}, P_l \mathbf{x}^{(l)} \rangle_A}{\langle P_l \mathbf{x}^{(l)}, P_l \mathbf{x}^{(l)} \rangle_X} = \lambda^{(l)}. \tag{3.13}$$

This provides a relation among the eigenvectors and eigenvalues of the operators in the multigrid hierarchy on all levels with the eigenvectors and eigenvalues of the finest-grid matrix pencil (A, X). Again one obtains the original formulation of the bootstrap setup cycle by choosing $X = I$ and by choosing $X = \widetilde{M}$ one obtains a setup cycle that yields approximations to the eigenvectors of the matrix pencil $(A, \widetilde{M})$. We note that the eigenvalue approximations in (3.13) are continuously updated within the algorithm so that the overall approach resembles an inverse Rayleigh-Quotient iteration found in eigenvalue computations (cf. [24]). For additional details of the algorithm and its implementation we refer to the paper [4].

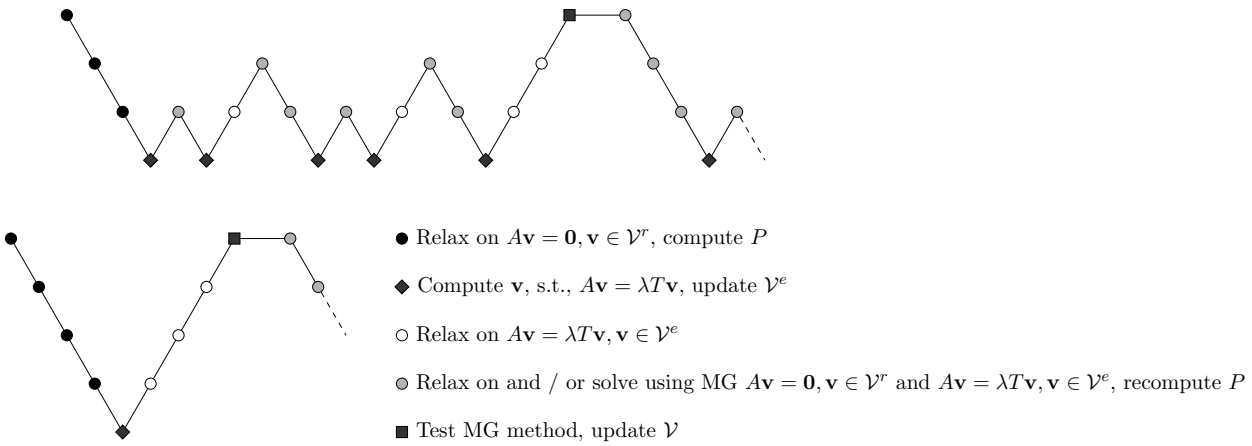

FIGURE 3.1. Galerkin Bootstrap AMG W-cycle and V-cycle setup schemes. Here, $\mathcal{V}^r$ denotes the set of relaxed vectors and $\mathcal{V}^e$ the set of vectors coming from the MGE process.

4. Numerical experiments

We consider four different test problems coming from discretizations of (1.2), corresponding to different distributions of the diffusion coefficient $a(x)$. The first two Problems P1 and P3 are ones where the interfaces of the jumps do not intersect, namely,

$$a(x) = \begin{cases} 1 & x \in \Omega_1 \ , \\ 10^{-k_{ij}} & x \in \Omega \setminus \Omega_1 \ , \end{cases} \tag{4.1}$$

where the domain Ω_1 corresponds to the one given by the white regions in the plot on the left in Figure 4.1. For problem P1, $k_{ij} = k \in \mathbb{Z}^+$ for all i, j, and for problem P3 $k_{ij} \in \{1, 2, \ldots, k\}$, where the values are selected randomly with uniform distribution (using built-in Matlab function `randi`). In the next two tests, Problems P2 and P4, we consider a checkerboard pattern for the distribution of the jumps, where now Ω_1 corresponds to the white regions in the plot on the right in Figure 4.1. For problem P2, the distribution in $\Omega \setminus \Omega_1$ is again uniform with $k_{ij} = k \in \mathbb{Z}^+$ for all i, j and for problem P4 we select the value k_{ij} randomly as in problem P3. We consider various k and as k grows the problems are more difficult.

We use a standard cell-centered finite volume method (see [14, 21]) for discretizing P1-P4 and choose a structured grid $0 = x_0 < x_1 < \cdots < x_{N+1}$, $x_i = \frac{i}{N+1}$, and $0 = y_0 < y_1 < \cdots < y_{N+1}$, $y_j = \frac{j}{N+1}$. Note that $h = h_x = h_y = \frac{1}{N+1}$. Here, each cell $[x_{i-1}, y_{j-1}] \times [x_i, y_j]$ is used as the control volume and the unknowns are located at each cell center $(x_{i-\frac{1}{2}}, y_{j-\frac{1}{2}}) = (x_{i-1} + \frac{h}{2}, y_{j-1} + \frac{h}{2})$. To define $a(x)$ on the interfaces of neighboring subdomains we use a harmonic average, e.g., for an interface S_* we have $a^- \neq a^+$ in general, where $a^- = a(x)$ in the volume on one side of the interface S_* and $a^+ = a(x)$ in the volume on the other side of S_*. We then write the discretized system as

$$a_e u_{i+1,j} + a_w u_{i-1,j} + a_n u_{i,j+1} + a_s u_{i,j-1} - (a_e + a_w + a_n + a_s) u_{i,j} = f_{i,j}, \tag{4.2}$$

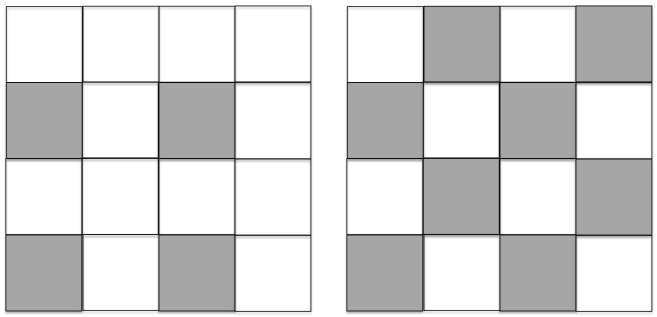

FIGURE 4.1. Distribution of the jump coefficient $a(x)$. Left: Distribution of P1 and P3; Right: Distribution of P2 and P4.

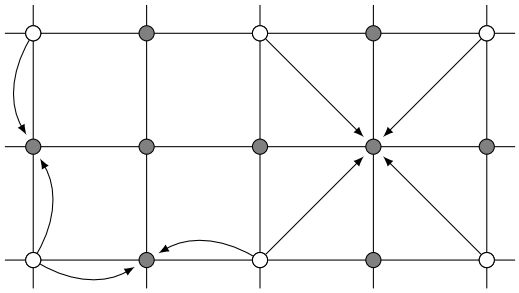

FIGURE 4.2. Full coarsening and interpolation relations ($\bullet$ F, $\circ$ C).

where $f_{i,j} = \int_V f \mathrm{d}V$ and V is the control volume $[x_{i-1}, y_{j-1}] \times [x_i, y_j]$ and a_* are harmonic averages of $a(x)$ on the two neighboring cells as in [19]. We assume Dirichlet boundary conditions and if an edge S_* is on the boundary of Ω, we set $u_{i+\frac{1}{2},j} = 0$.

4.1. **Compatible relaxation: measuring the quality of C.** We begin with tests that compare the standard F-relaxation form of CR in (3.5), the estimate of $E_{TG}(P_\circ)$ obtained by using the identity in (3.6) to apply the coarse-grid correction with ideal interpolation ($P = P_\circ$), and the spectral radius of $E_{TG}(\tilde{P}_\sharp)$, that is, the two-grid method with optimal interpolation, for Problems P1-P4. In all tests, we use forward Gauss-Seidel for pre-smoothing and backward Gauss-Seidel for post-smoothing in defining the symmetrized two-grid error propagation operator

$$E_{TG}(P) = (I - M^{-1}A)(I - \Pi_A(P))(I - M^{-T}A), \tag{4.3}$$

and we consider standard full-coarsening ($h \to 2h$, see Figure 4.2) to define the coarse variable set $C \subset \{1, ..., n\}$ for different choices of the problem size $n = N \times N$.

The results of these tests for various values of the jump discontinuity defined by parameter k are given in Table 4.1. The table at the top contains approximations of the spectral radius of $E_{TG}(P_\circ)$. The second table contains estimates of the two-grid convergence rate obtained by running 5 steps of the iteration (3.6) starting with a random initial guess, where the action of A_{ff}^{-1} in (3.6) is approximated by $L = 2$ diagonally preconditioned Conjugate Gradient iterations. Here, we combine the iteration (3.6) with Gauss Seidel pre- and post-smoothing, which then mimics the two-grid method with ideal $P = P_\circ$. The third table contains results of the F-relaxation form of CR for symmetric Gauss Seidel, again assuming full coarsening

as the choice of C. And the bottom table contains results of the two-grid method with optimal interpolation, $\tilde{P}_\sharp$.

Spectral radius of $E_{TG}(P_\circ)$ in (4.3)

	$k=1$				$k=2$				$k=4$				$k=8$			
Size	P1	P2	P3	P4	P1	P2	P3	P4	P1	P2	P3	P4	P1	P2	P3	P4
16^2	.259	.255	.300	0.397	.251	.251	.297	.535	.250	.250	.298	.577	.250	.250	.294	.679
32^2	.260	.256	.302	0.445	.251	.251	.301	.649	.250	.250	.293	.791	.250	.250	.285	.887
64^2	.261	.256	.303	0.473	.251	.251	.301	.714	.250	.250	.294	.879	.250	.250	.292	.991
128^2	.261	.256	.305	0.471	.251	.251	.301	.729	.250	.250	.298	.924	.250	.251	.294	.997

Approximation of $E_{TG}(P_\circ)$ in (4.3) using identity (3.6)

	$k=1$				$k=2$				$k=4$				$k=8$			
Size	P1	P2	P3	P4	P1	P2	P3	P4	P1	P2	P3	P4	P1	P2	P3	P4
16^2	.240	.235	.249	.209	.233	.231	.244	.210	.232	.231	.239	.217	.232	.231	.231	.225
32^2	.245	.243	.253	.198	.241	.241	.250	.204	.240	.241	.247	.205	.240	.241	.239	.220
64^2	.244	.242	.252	.200	.239	.239	.250	.205	.239	.239	.247	.216	.239	.239	.237	.225
128^2	.234	.237	.220	.202	.240	.240	.231	.206	.240	.240	.236	.214	.240	.240	.238	.223

Compatible Relaxation iteration (3.5) with symmetric Gauss Seidel

	$k=1$				$k=2$				$k=4$				$k=8$			
Size	P1	P2	P3	P4	P1	P2	P3	P4	P1	P2	P3	P4	P1	P2	P3	P4
16^2	.242	.176	.512	.693	.075	.052	.493	.839	.007	.005	.499	.937	7e-5	5e-5	.500	.999
32^2	.243	.177	.524	.786	.075	.052	.520	.939	.007	.005	.516	.995	7e-5	5e-5	.512	1.00
64^2	.244	.177	.530	.777	.075	.052	.527	.927	.007	.005	.522	.989	7e-5	5e-5	.515	1.00
128^2	.244	.178	.533	.790	.075	.052	.526	.951	.007	.005	.523	.998	7e-5	5e-5	.517	1.00

Spectral radius of $E_{TG}(P_\sharp)$ in (4.3)

	$k=1$				$k=2$				$k=4$				$k=8$			
Size	P1	P2	P3	P4	P1	P2	P3	P4	P1	P2	P3	P4	P1	P2	P3	P4
16^2	.041	.024	.124	.132	.005	.002	.108	.120	5e-5	3e-5	.102	.102	5e-9	2.5e-9	.065	.065
32^2	.042	.024	.134	.148	.005	.002	.131	.140	5e-5	3e-5	.126	.128	5e-9	2.5e-9	.087	.117
64^2	.042	.024	.137	.154	.005	.002	.136	.152	5e-5	3e-5	.132	.146	5e-9	2.5e-9	.124	.151
128^2	.042	.024	.140	.160	.005	.002	.139	.159	5e-5	3e-5	.136	.157	5e-9	2.5e-9	.127	.159

TABLE 4.1. Spectral radius of two-grid methods with ideal interpolation (top), using CG to approximate A_{ff}^{-1} (top-middle), results for compatible relaxation (bottom-middle) and with optimal interpolation (bottom), applied to Problems P1-P4 (with symmetric GS as smoother).

Overall, we see that CR convergence rates are acceptable for all problems and choices of the problem parameters except for Problem P4. Moreover, from the results obtained in the middle table it is clear that one can obtain an accurate estimate of $E_{TG}(P_\circ)$ using (3.6) with a small number of inner PCG iterations to approximate A_{ff}^{-1}, again in all cases except for Problem P4. This poor performance observed for Problem P4 is of course expected since in this case the convergence of F-relaxation with full coarsening is $\rho > .9$ and so A_{ff} may not be well conditioned in the sense of the bound given in (3.7). In general, these results suggest that full coarsening may not be a good choice for Problem P4. However, as can be seen in the next set of experiments (in the bottom table), with optimal interpolation full coarsening does give acceptable results. The rapid convergence observed in these tests, especially for Problem P4, can be explained by considering the results provided in Figure 4.3, which contains plots of the spectra of A and $(A, \widetilde{M})$ for various tests with $N = 16$.

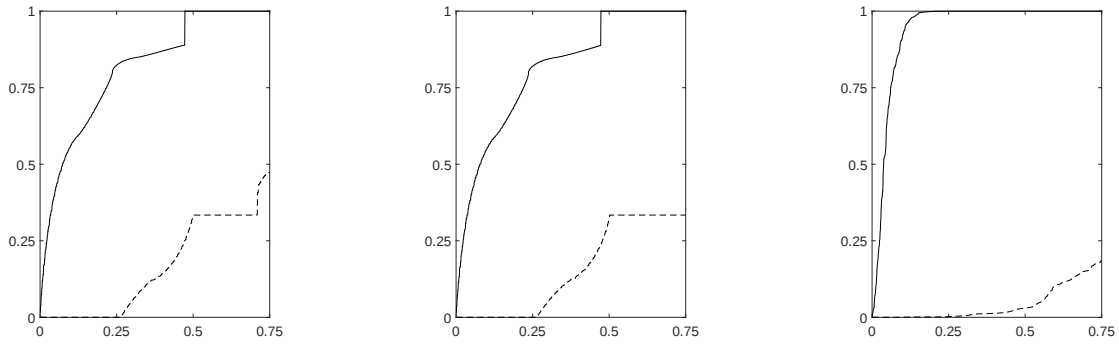

FIGURE 4.3. Lower $\frac{3}{4}$ of the spectra of $(A, \widetilde{M})$ (solid line) and A (dashed line), which is scaled by $\lambda_{\max}(A)$. (left) Lex. Gauss-Seidel for P1 ($k = 4$, 35×35); (center) Lex. Gauss-Seidel for P2 ($k = 4$, 35×35); (right) Red-black block Gauss-Seidel with 5×5 blocks for P4 ($k = 4$, 35×35).

Here, we see that the eigenvalues of $(A, \widetilde{M})$ vary substantially from the eigenvalues of A, e.g. in the right plot for Problem P4, less than $\frac{n}{4}$ of the generalized eigenvalues are different from 1. Thus, for our choice of full coarsening with $n_c = \frac{n}{4}$, we obtain very fast convergence. This behavior for the optimal interpolation operator is in fact expected since this operator minimizes the two-grid convergence rate directly, whereas the ideal interpolation operator is only a minimizer of an upper bound on the convergence rate.

Similarly, the convergence factors (or spectral radii) of compatible relaxation are essentially zero or one for some of the tests. For the F-relaxation form of the compatible relaxation iteration, it is known that its spectral radius only gives a qualitative measure of the quality of the given coarse gird, C. Moreover, the convergence rate of CR can often substantially under-estimate the performance of the two-grid method with ideal interpolation. This is true, for example, for the results reported for test problems P1 and P2, where we see that CR rates substantially underestimate the performance of the two-grid method with ideal interpolation, $P_\circ$. It is also true for the five-point central difference Poisson problem and Gauss Seidel smoothing, where, with a red-black coarse grid this F-relaxation form of CR has a spectral radius equal to zero, but the resulting two-grid method with full smoothing and ideal interpolation converges at a rate of about $\rho = .2$. Hence, a uniform convergence rate with this choice of CR gives an indication that the choice of the coarse grid C is suitable, but it can not in general accurately predict the two-grid convergence with ideal interpolation. This observation is further illustrated in the results where we use the approximation of $E_T G(P_\circ)$ in (4.3) using identity (3.6), which does give accurate results.

We note that if we instead consider red-black coarsening for problem P4, then F-relaxation becomes an exact solve, i.e., the spectral radius of the CR iteration, $\rho_s = 0$. In addition, when using the same red-black coarsening and iteration (3.6), again with 2 inner PCG iterations, we obtain an estimate of the spectral radius of $\rho = .248$ for Problem P4 with $k = 8$ and $h = 1/2^5$, where the true spectral radius of the two-level method is .250 independent of k and h. Thus, in practice, one can run F-relaxation to choose C until the CR iteration converges quickly (so that A_{ff} is well conditioned by (3.7)) and then compute the sharp estimate of $E_{TG}(P_\circ)$ defined in terms of (3.6) using PCG iterations to approximate the action of A_{ff}^{-1}

in (3.6) in order to obtain a more accurate estimate of the convergence rate of the two-grid method using ideal interpolation.

Finally, in Section 3, we showed that in general the two-level method with optimal interpolation will converge faster than the method with ideal interpolation. Here, we observe these results numerically for Problems P1-P4. Overall, we observe that the reported convergence results are consistent with the theoretical result that $\rho(E_{TG}(P_\sharp)) \leq \rho(E_{TG}(P_\star))$ and for Problems P2 and P4 a significant improvement is observed. We note that for the Poisson problem (i.e., $k = 0$), the two-grid method with optimal P and full coarsening has its spectral radius bounded by .14 independent of the problem size n.

4.2. **Compatible relaxation with optimal interpolation.** As discussed in Section 3.1, the convergence rate of the F-relaxation form of compatible relaxation can be used to measure the quality of the coarse variable set in that it bounds the $\min - \max$ solution $\mu^\star_{\widetilde{M}}$ in (2.8). Recall that this construction assumes the ideal interpolation operator in (2.13), which as we showed above does not give the best choice of the classical AMG form of interpolation due to the forms of R and S given in (2.10) that are assumed in this setting.

Our aim in this section is to study the use of CR together with the optimal forms of R and S given in Lemma 3, namely, $\tilde{R}_\sharp = (\tilde{P}_\sharp P_c P_c^T)^T \widetilde{M}$ and $S_\sharp = \begin{pmatrix} \mathbf{v}_{n_c+1} & \cdots & \mathbf{v}_n \end{pmatrix}$, which leads to the optimal interpolation matrix as the minimizer of $\mu_{\widetilde{M}}$. Here, P_c defines the matrix used in deriving the classical AMG form of $P_\sharp$ given in (2.7):

$$\tilde{P}_\sharp = P_\sharp P_c^{-1} = \begin{bmatrix} P_f P_c^{-1} \\ I \end{bmatrix}, \quad P_\sharp = \begin{bmatrix} P_f \\ P_c \end{bmatrix} \leftarrow \begin{bmatrix} \mathbf{v}_1 & \cdots & \mathbf{v}_{n_c} \end{bmatrix},$$

with the set C chosen such that P_c is non-singular. The arrow notation is used to denote that $P_\sharp$ with columns consisting of the smallest n_c eigenvectors of the generalized eigenproblem for $(A, \widetilde{M})$ is reordered according to the $C - F$ splitting of the unknowns. Note that from Lemma 2 we have that $\tilde{P}_\sharp$ not only yields the optimal two-grid convergence rate, i.e., it gives $\kappa_\sharp$ in (2.3), it also minimizes the approximation property $\mu_{\widetilde{M}}$ with respect to P.

Given the above choice of $S = S_\sharp$ we have that the spectral radius of CR is given by (see (3.9))

$$\rho_{S_\sharp}(I - \widetilde{M}_{S_\sharp}^{-1} A_{S_\sharp}) = 1 - \lambda_{n_c+1}. \tag{4.4}$$

Here, $\widetilde{M}$ denotes the symmetric Gauss-Seidel smoother. Note that, the CR rate gives the same result as the convergence rate of the two-grid method with optimal interpolation, namely, the same rate obtained with $\kappa_\sharp$. However, unlike the simplified F-relaxation version of CR given in (3.5), the convergence rate of this form of CR does not depend on the actual coarse points that are chosen, instead it only depends on the cardinality of the coarse variable set $n_c = |C|$. The choice of the coarse variable set now defines the matrix P_c that is used in constructing the classical AMG form of optimal interpolation. Hence, in this setting we can use CR to determine the number of coarse points that are required in order to achieve a convergence rate of the resulting two-grid method and then we choose the set C so that P_c is well conditioned.

The problem of finding a well-conditioned submatrix P_c can be viewed as finding a subset of n_c columns of $P_\sharp^T$ that form a well conditioned basis of $\mathbb{R}^{n_c}$ or in looser terms a set of n_c columns that are as linearly independent as possible. Besides the condition number of the basis, i.e., a measure for its orthogonality, another natural formalization of this question

is the volume of the parallelepiped spanned by the bases. In the case that all columns of $P_\sharp^T$ have comparable norm, a maximal volume (determinant) basis has a small condition number and vice versa. Unfortunately, finding the maximal volume submatrix is an NP-hard problem (cf. [26]), but there exists a greedy algorithm (cf. Algorithm 1) that is able to find a sub-matrix P_c with locally maximal determinant (see [18, 17] for details). Even though there is no guarantee that the submatrix found in this way has a small condition number, we find in practice that the large eigenvalues tend to stay within the same order. In contrast, the nearly zero eigenvalues of P_c move away from the origin significantly when the algorithm is applied to some random initial choice of coarse grid.

Figures 4.4 - 4.6 contain results of the algorithm applied to our scalar diffusion problem in (1.2) for different choices of the diffusion tensor $a(x)$, namely, the distribution for our test problems P1-P4 with $k = 4$. For all tests we use a discretization of the problem with 35×35 finite volumes. Each figure contains plots of the choice of coarse variable set C, denoted by the black circles as well as the volume and condition numbers of the depicted choice of C. We depict the initial (random) choice of the C set and the set determined by the `maxvol` algorithm. Further, we show a plot of the convergence rate versus the cardinality of $n_c = |C|$, and plots of three (randomly chosen) columns of the resulting optimal classical AMG form of interpolation that we obtain for the given coarse grid and then computing $\tilde{P}_\sharp$ by multiplying $P_\sharp$ by P_c^{-1}. We observe that, in all tests, the set of coarse variables properly aligns with the choice of $a(x)$ and the given smoother. For example, in Figure 4.5 we naturally obtain standard full coarsening. And for the results in Figure 4.6 for Problem P4, when using a non-overlapping red-black ordered block Gauss Seidel smoother (with 5×5 blocks) we see that the coarse points largely lie on the boundaries of the subdomains, as expected. In addition, the plots of the convergence rates are given on the top right and allow one to choose $n_c = |C|$ with a guaranteed lower bound on the convergence rate of the resulting two-grid method, namely the one obtained with $\tilde{P}_\sharp$. Finally, we note that the columns of the resulting optimal classical AMG form of interpolation are highly localized for all test problems as shown in the bottom rows of plots in Figures 4.4 - 4.6.

Algorithm 1: `maxvol` coarse variable selection – Input: $P_\sharp$ and n_c, Output: C, F

Choose initial set C such that $|C| = n_c$, set $X := (P_\sharp)_C$

Calculate $\tilde{P}_\sharp := \pi P_\sharp X^{-1} = \begin{pmatrix} I \\ W \end{pmatrix}$ `// reordered according to` C`-`F`,` π `: row permutation`

while $\max_{i,j} |(\tilde{P}_\sharp)_{i,j}| > 1$

- $(i', j') = \text{argmax}\{|(\tilde{P}_\sharp)_{i,j}|\}$ `//` $i > n_c$`, i.e.,` $i \notin C$
- Set $C = (C \setminus \{j'\}) \cup \{i'\}$ `// swap rows` j' `and` i'
- Update $\tilde{P}_\sharp$ `//rank one updates based on Sherman-Morrison formula`

4.3. **Bootstrap AMG and the generalized eigenproblem.** To illustrate the effect of the choice of T_l in the MGE bootstrap process, we provide results in which a W^2-cycle bootstrap setup using four forward Gauss Seidel pre- and four backward Gauss Seidel post-smoothing steps to compute the set of relaxed vectors $\mathcal{V}^r$ and set of bootstrap vectors $\mathcal{V}^e$ coming from the MGE process, with $k_r = |\mathcal{V}^r| = 8$ and $k_e = |\mathcal{V}^e| = 8$, respectively. The sets $\mathcal{V}^r$ and $\mathcal{V}^e$ are then combined to form the set of TVs $\mathcal{V}$ that is used to compute the least

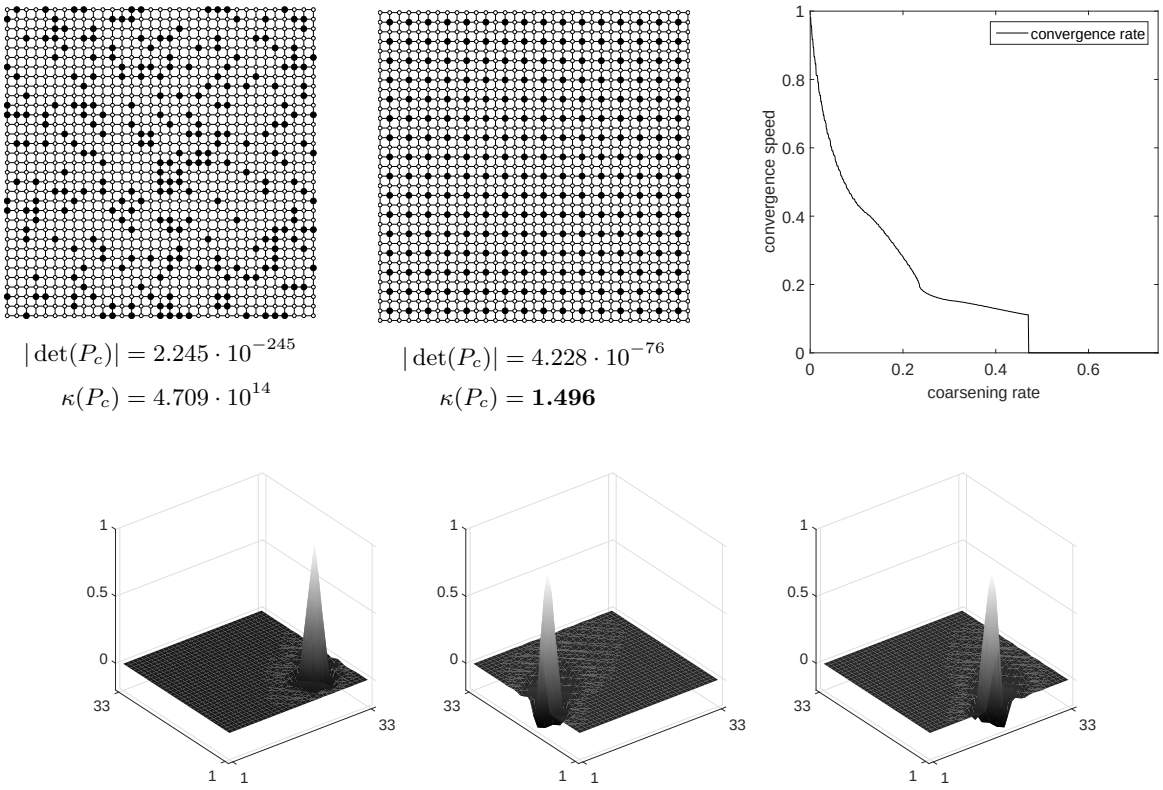

FIGURE 4.4. Lexicographic Gauss-Seidel for $P1$ ($k = 4$, 35×35, $n_c = 289$). (top left) initial random choice of C; (top center) C determined by `maxvol`; (top right) CR rate $\rho_{S_\sharp} = 1 - \lambda_{n_c+1}$ w.r.t. ratio $\frac{n_c}{n}$; (bottom row) columns of $\tilde{P}_\sharp$ with C from `maxvol`

squares interpolation operator on each level. In these tests, only relaxation is applied to the homogenous systems in both setup cycles to update the sets $\mathcal{V}^r$. We use forward Gauss Seidel as a pre-smoother and backward Gauss Seidel as the post-smoother in the solve phase as well. The coarse grids and sparsity structure of interpolation are defined as in the previous tests on all levels, i.e., by full coarsening and nearest neighbor interpolation as depicted in Figure 4.3, and the problem is coarsened to a coarsest level with $h = 1/8$.

The results of our experiments are given in Table 4.2. Here, we observe that using the generalized eigen-problem in the BAMG setup gives uniformly better results, than just working with eigen-approximations of A. In addition, if we compare the results obtained in the left table with the results given earlier (see Table 4.1), then we see that the multilevel BAMG approach (with sparse P) converges faster than the two-level method that uses the ideal interpolation operator.

5. Conclusion

In this paper, we introduced an classical form of optimal AMG interpolation and a measure of the quality of the coarse variable set that gives precise estimates of the convergence rate of two-grid method with this optimal choice of interpolation, which is based on eigenvectors of the generalized eigen-problem involving the system matrix and its associated symmetrized

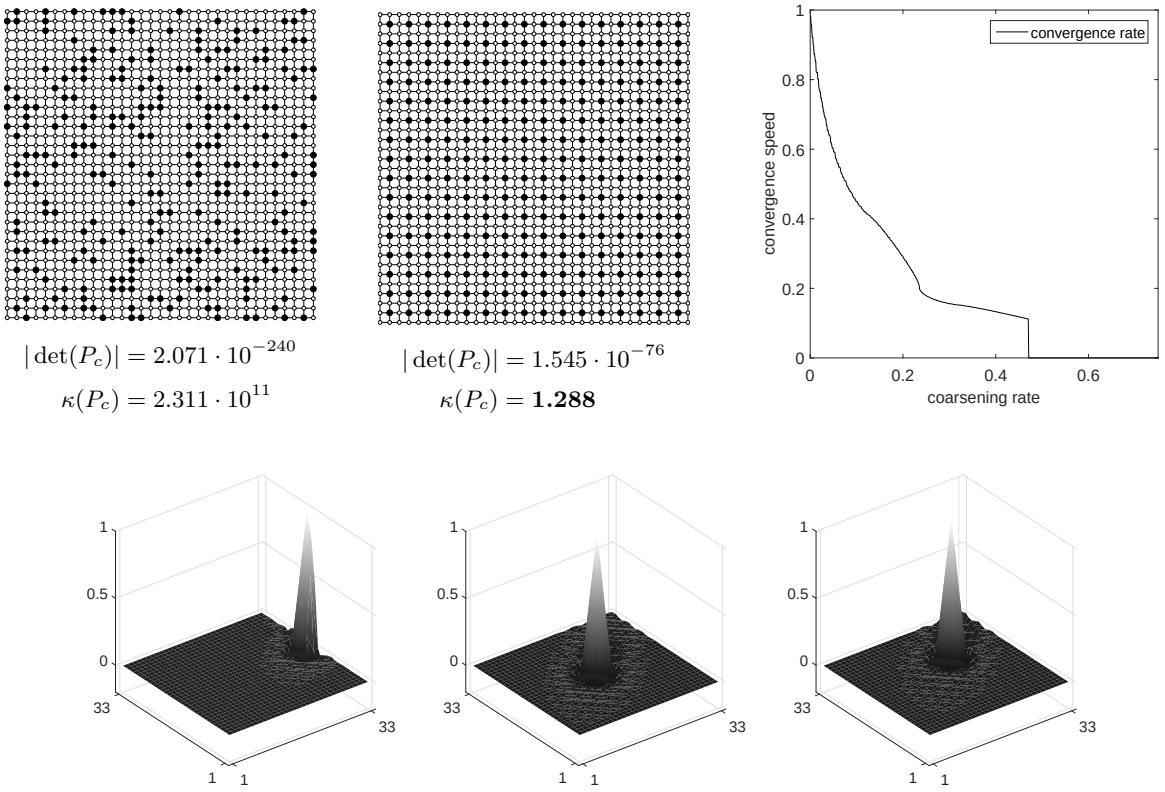

FIGURE 4.5. Lexicographic Gauss-Seidel for $P2$ ($k = 4$, 35×35, $n_c = 289$). (top left) initial random choice of C; (top center) C determined by `maxvol`; (top right) CR rate $\rho_{S_\sharp} = 1 - \lambda_{n_c+1}$ w.r.t. ratio $\frac{n_c}{n}$; (bottom row) columns of $\tilde{P}_\sharp$ with C from `maxvol`

Size / k	1	2	4	8
17^2	.276	.377	.398	.626
33^2	.260	.256	.302	.445
65^2	.261	.256	.299	.427
129^2	.261	.256	.299	.427

Size / k	1	2	4	8
17^2	.357	.592	.405	.966
33^2	.416	.591	.302	.953
65^2	.261	.256	.303	.573
129^2	.261	.256	.305	.571

TABLE 4.2. BAMG setup results for Problem P4 with $X = \widetilde{M}$ (left) and $X = I$ (right).

smoother. We showed numerically that in the case of full smoothing the convergence rates of the two-grid method with this optimal interpolation can converge much faster than the method with ideal interpolation, assuming a standard choice of the coarse variable type. We also showed that for full smoothing and a proper choice of the coarse variables, the optimal and ideal interpolation matrices have the same range. Finally, using these new results we designed a generalized bootstrap AMG setup algorithm that incorporates this generalized eigen-problem and illustrated the utility of the approach when applied to a scalar diffusion

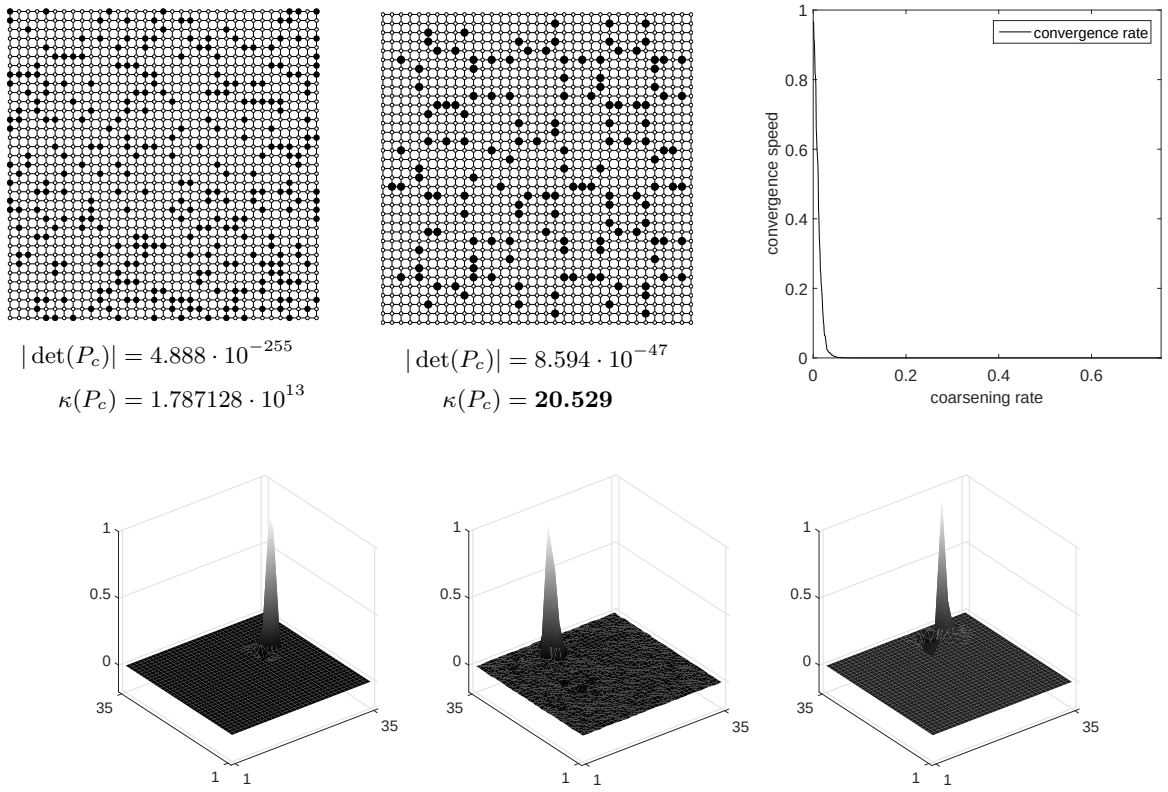

FIGURE 4.6. Red-black block Gauss-Seidel for $P4$, 5×5 blocks ($k = 4$, 35×35, $n_c = 144$). (top left) initial random choice of C; (top center) C determined by `maxvol`; (top right) CR convergence rate $\rho_{S_\sharp} = 1 - \lambda_{n_c+1}$ w.r.t. ratio $\frac{n_c}{n}$; (bottom row) three columns of $\tilde{P}_\sharp$ with C from `maxvol`

problem with highly varying diffusion coefficient. Numerically, we observed that the BAMG method (spanning multiple levels) with sparse P outperforms the two-grid method with the ideal P (which is a dense matrix). Overall, our initial analysis and numerical tests show that for certain problems the optimal interpolation operator can give much better performance than the ideal one and it be approximated in practice by a sparse matrix. Together, these findings suggest that the use of optimal interpolation can lead to new insights in AMG methods and it's use needs to be studied in more detail. We mention that in our tests of the BAMG algorithm we did not use strength of connection in defining the sparsity structure of interpolation, instead we simply limited interpolation to nearest neighbors defined in terms of the geometry. The use of strength of connection in choosing the coarse grid and sparsity of interpolation is another idea that we intend to study in detail in the future. In addition, we note that, though we considered only point Gauss Seidel as a smoother in this paper, we are in the process of studying these results for block smoothers in the context of coupled PDE systems.

References

[1] A. Brandt. General highly accurate algebraic coarsening. *ETNA*, 10:1–20, 2000. Special issue on the Ninth Copper Mountain Conference on Multilevel Methods.

[2] A. Brandt. Multiscale scientific computation: review 2001. In T. J. Barth, T. F. Chan, and R. Haimes, editors, *Multiscale and Multiresolution Methods: Theory and Applications*, pages 1–96. Springer, Heidelberg, 2001.

[3] A. Brandt, J. Brannick, , K. Kahl, and I. Livshits. Bootstrap AMG: status, open problems and outlook. *Journal of Numerical Mathematics: Theory, Methods and Applications*, 8(1):112–135, 2015.

[4] A. Brandt, J. Brannick, K. Kahl, and I. Livshits. Bootstrap AMG,. *SIAM Journal of Scientific Computing*, 33:612–632, 2011.

[5] A. Brandt, S. McCormick, and J. Ruge. Algebraic multigrid (AMG) for automatic multigrid solution with application to geodetic computations. Technical report, Colorado State University, Fort Collins, Colorado, 1983.

[6] A. Brandt, S. McCormick, and J. Ruge. Algebraic multigrid (AMG) for sparse matrix equations. In *Sparsity and its applications (Loughborough, 1983)*, pages 257–284. Cambridge Univ. Press, Cambridge, 1985.

[7] J. Brannick and R. Falgout. Compatible relaxation and coarsening in algebraic multigrid. *SIAM J. Sci. Comp.*, 32(3):1393–1416, 2010.

[8] J. Brannick and K. Kahl. Bootstrap AMG for the Wilson Dirac system. *SIAM Journal of Scientific Computing*, 36(3):321–347, 2014.

[9] J. Brannick, K. Kahl, and I. Livshits. Algebraic distances as a measure of AMG strength of connection for anisotropic diffusion problems. *Electronic Transactions in Numerical Analysis*, 44:472–496, 2015.

[10] J. Brannick, K. Kahl, and S. Sokolovic. An adaptively constructed algebraic multigrid preconditioner for irreducible markov chains. *Journal of Applied Numerical Mathematics*. Submitted January 19, 2015, arXiv:1402.4005.

[11] J. Brannick and L.Zikatanov. Algebraic multigrid methods based on compatible relaxation and energy minimization. In *Proceedings of the 16th International Conference on Domain Decomposition Methods*, volume 55 of *Lecture Notes in Computational Science and Engineering*, pages 15–26. Springer, 2007.

[12] M. Brezina, R. Falgout, S. MacLachlan, T. Manteuffel, S. McCormick, and J. Ruge. Adaptive smoothed aggregation αSA. *SIAM J. Sci. Comput.*, 25:1896–1920, 2004.

[13] M. Brezina, R. Falgout, S. MacLachlan, T. Manteuffel, S. McCormick, and J. Ruge. Adaptive algebraic multigrid. *SIAM J. Sci. Comput.*, 27(4):1261–1286 electronic, 2006.

[14] Robert Eymard, Thierry Gallouët, and Raphaèle Herbin. Finite volume methods. *Handbook of numerical analysis*, 7:713–1018, 2000.

[15] R. Falgout, P. Vassilevski, and L. Zikatanov. On two–grid convergence estimates. *Numerical Linear Algebra with Applications*, 12(5-6):471–494, 2005.

[16] R. D. Falgout and P. S. Vassilevski. On generalizing the AMG framework. *SIAM J. Numer. Anal.*, 42(4):1669–1693, 2004. UCRL-JC-150807.

[17] S. A. Goreinov, I. V. Oseledets, D. V. Savostyanov, E. E. Tyrtyshnikov, and N. L. Zamarashkin. *How to Find a Good Submatrix*, pages 247–256. World Scientific, April 2010.

[18] Donolad E Knuth. Semi-optimal bases for linear dependencies. *Linear and Multilinear Algebra*, 17(1):1–4, 1985.

[19] C. Liu, Z. Liu, and S. McCormick. An efficient multigrid scheme for elliptic equations with discontinuous coefficients. *Communications in Applied Numerical Methods*, 8:621–631, 1992.

[20] Jan Mandel, Marian Brezina, and Petr Vanek. Energy optimization of algebraic multigrid bases. 1998. CU Denver Technical Report.

[21] Alexander A Samarskii. *The theory of difference schemes*, volume 240. CRC Press, 2001.

[22] P. Vaněk, J. Mandel, and M. Brezina. Algebraic multigrid by smoothed aggregation for second and fourth order elliptic problems. *Computing*, 56:179–196, 1996.

[23] W. L. Wan, Tony F. Chan, and Barry Smith. An energy-minimizing interpolation for robust multigrid methods. *SIAM J. Sci. Comp.*, 21(4):16321649, 2000.

[24] J. Wilkinson. The algebraic eigenvalue problem. Clarendon Press, Oxford, 1965.

[25] J. Xu and L. Zikatanov. Algebraic multigrid methods. article: arXiv:1611.01917.

[26] Ali ivril and Malik Magdon-Ismail. Exponential inapproximability of selecting a maximum volume submatrix. *Algorithmica*, 65(1):159, 2013.